



# Antiproton-Ion-Collider

A Tool for the measurement of both neutron and proton rms radii

P. Kienle, SMI, Wien and TU, München

- Motivation
- Medium energy antiproton absorption
- Antiproton-Ion-Collider
- Cross section measurements
- N/P rms radii,  $c$  and  $a$  determination

[1] P. Kienle, Nucl. Instr. Meth. B 214 (2004) 191.

[2] H. Lenske and P.Kienle, arXiv:nucl.th/05022065v1, 25.Feb.2005

[3] AIC Technical Proposal to GSI January 2005



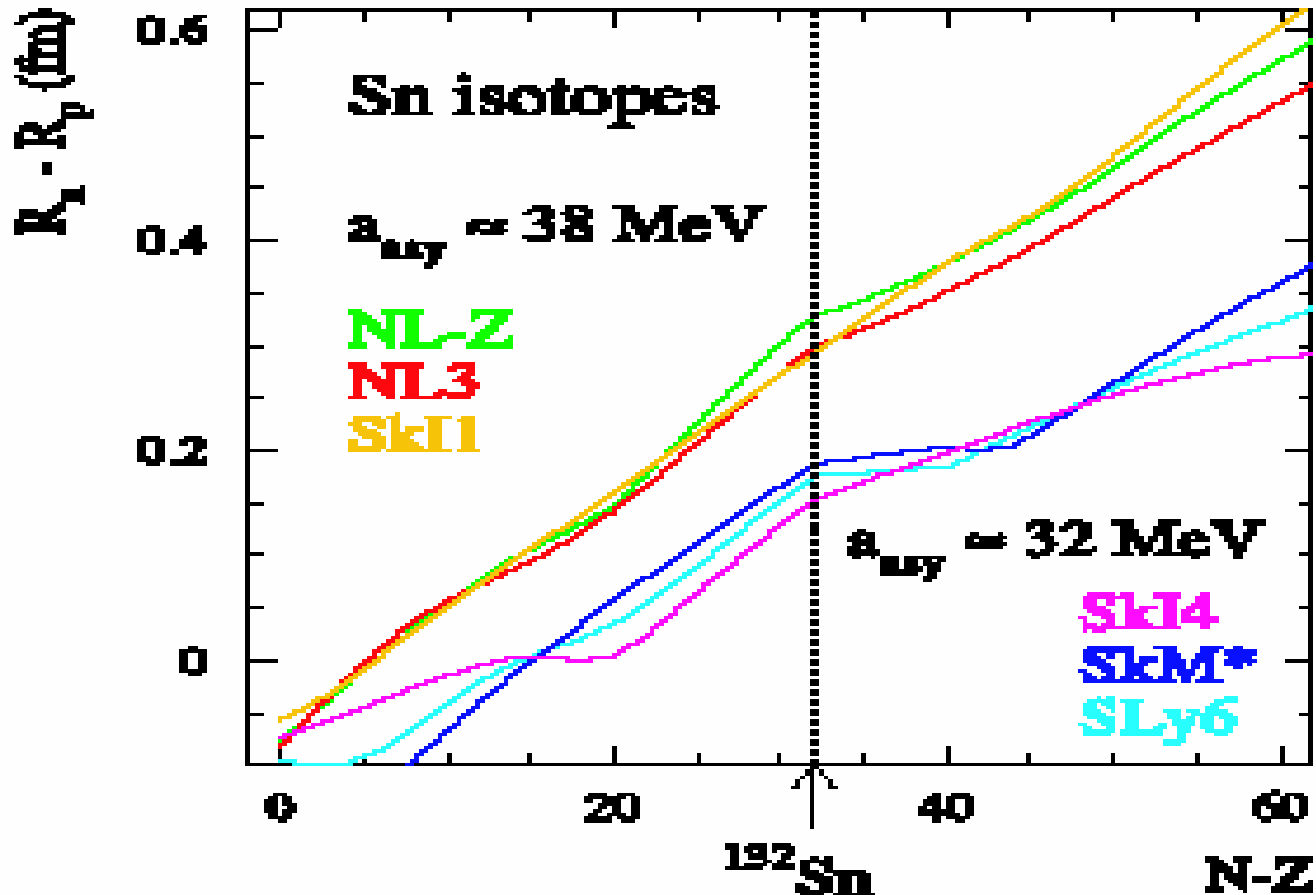
# AIC Concept

- 30-100 MeV Antiproton–740A A MeV Ion(variable)
- Modification of e-ion collider
- Addition of antiproton injection and cooling up to  $T=100$  MeV
- Fragment detection by Schottky mass spectroscopy and magnetic analysis in NESR
- Luminosity monitor by detection of Rutherford scattered antiprotons



# Differences in Neutron and Proton Radii for Sn-Isotopes

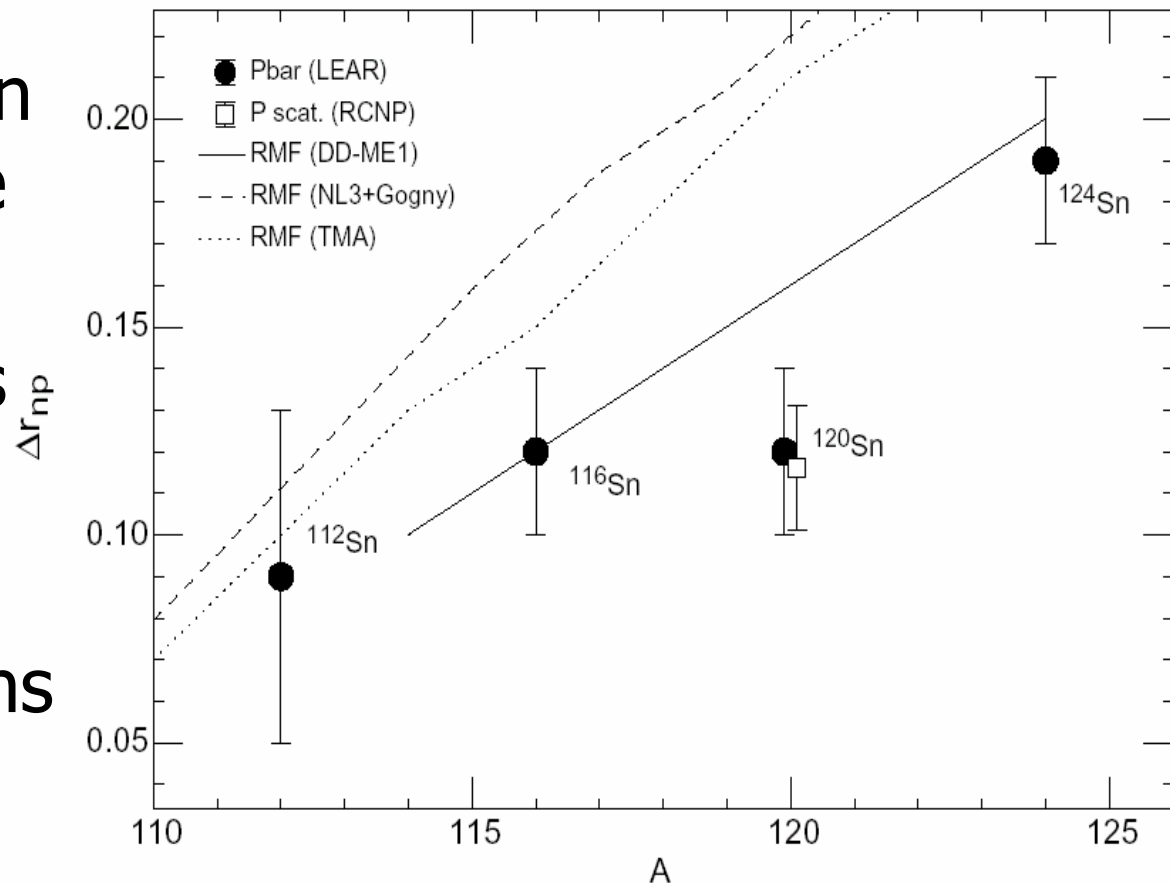
## Theoretical predictions





# Experimental Methods for rms Radii Differences

- Electron and Proton Scattering, Isotope Shift
- Antiprotonic Atoms
- Charge Exchange Reactions
- Knock-out Reactions



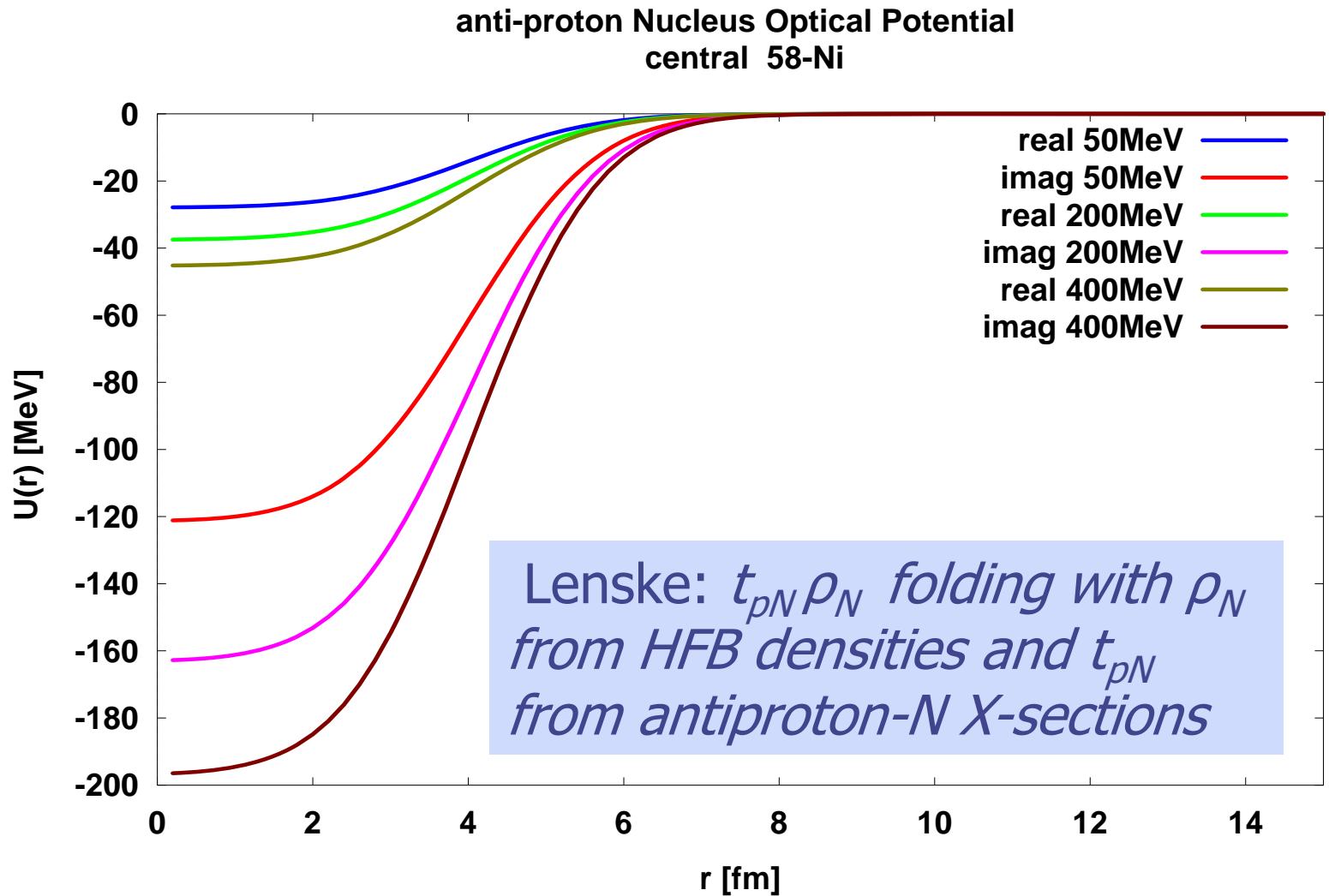


# Antiproton Absorption on Neutrons or Protons

- Yields of A-1 isobars with (N-1) or (Z-1) from atomic antiproton absorption
- Absorption radius undefined
- Not directly applicable for RI-beam-nuclei
- Yields of A-1 Isobars with (N-1) or (Z-1) from medium energy antiproton absorption
- Absorption proportional to  $\langle r^2 \rangle_n$  and  $\langle r^2 \rangle_p$  respectively at high enough energies
- From energy dependence of absorption,  $c_n$ ,  $a_n$ ,  $c_p$ ,  $a_p$  of Fermi distribution



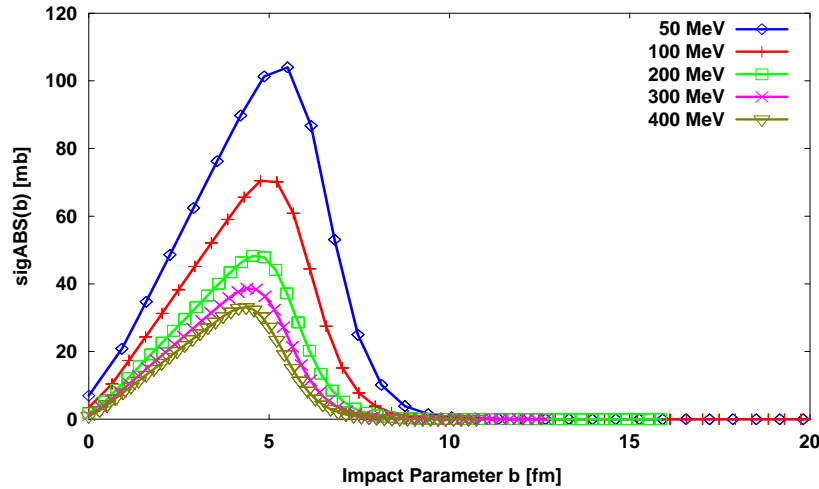
# Antiproton optical potential, $^{58}\text{Ni}$



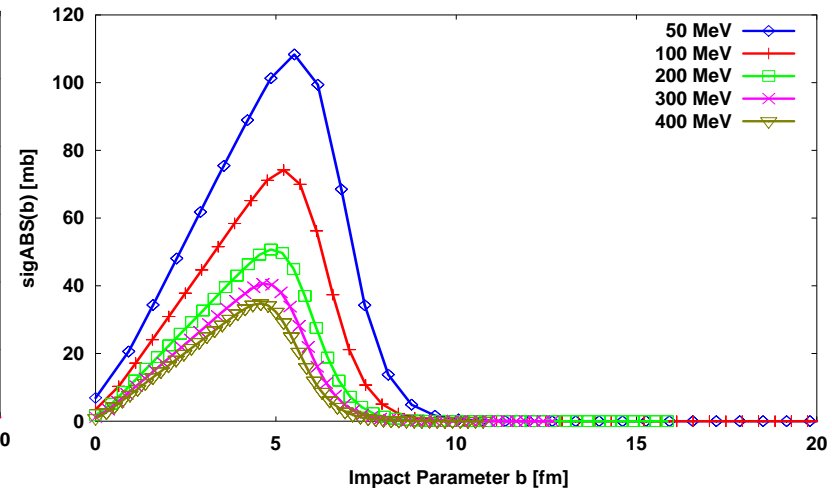


# Impact Parameter Dependence

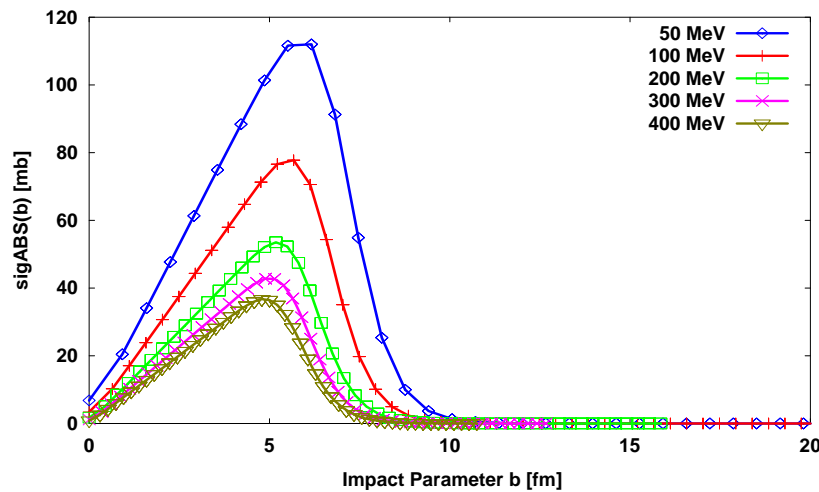
Antiproton-Nucleus Partial Absorption Cross Section  
48Ni



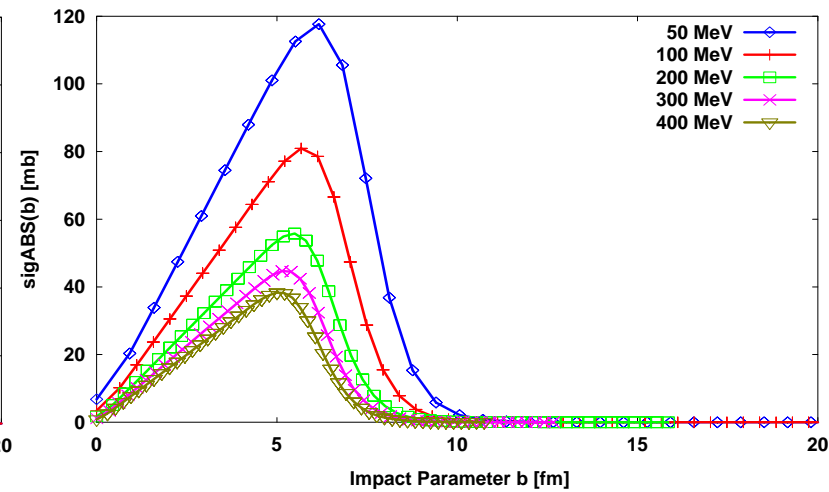
Antiproton-Nucleus Partial Absorption Cross Section  
58Ni



Antiproton-Nucleus Partial Absorption Cross Section  
68Ni

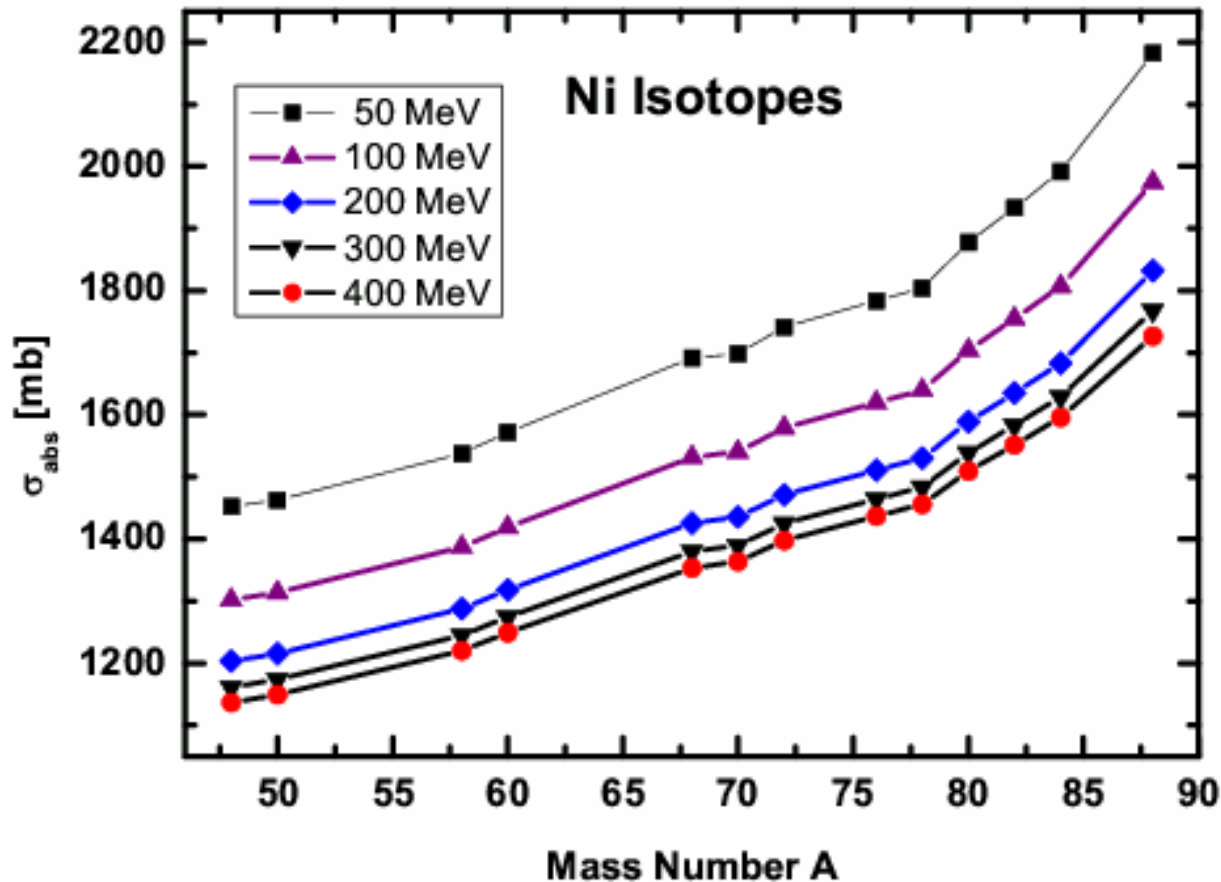


Antiproton-Nucleus Partial Absorption Cross Section  
78Ni





# Energy Dependence of Absorption in Ni

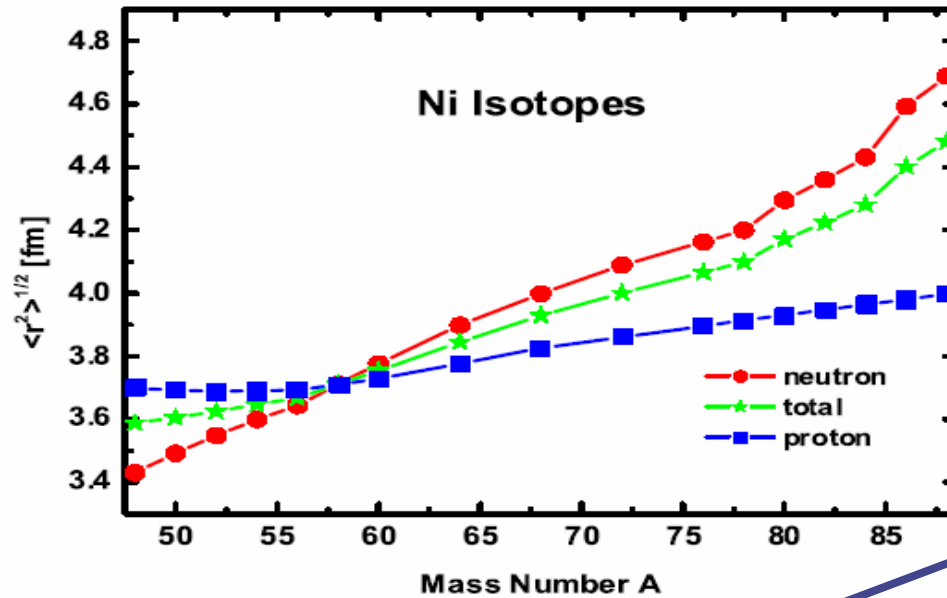


- At high energies X-section saturates at geometrical limit
- At lower energies tails of nucleons contribute





# $\langle r^2 \rangle_{t,n,p}$ and $\sigma_{t,n,p}$ for Ni Isotopes

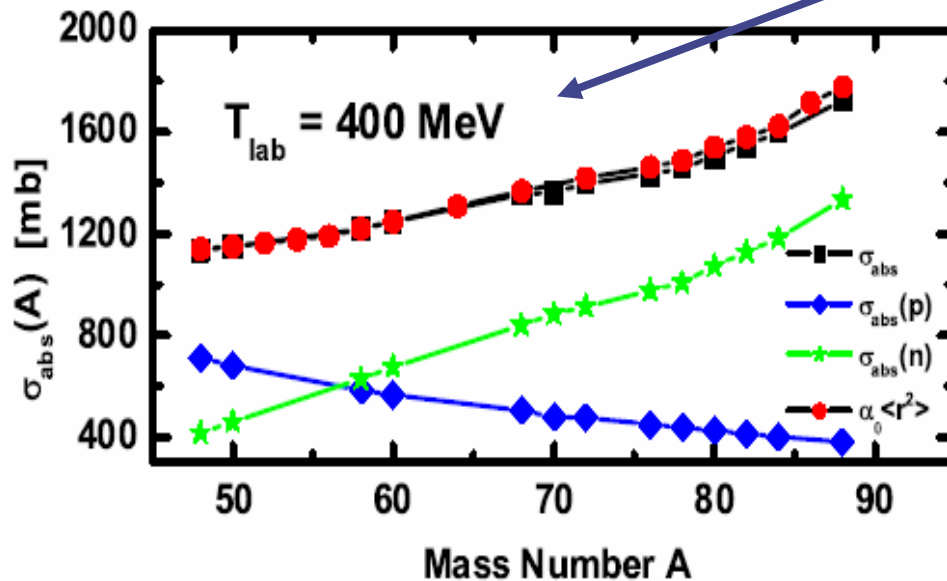


$$\sigma_R^{total} = C \langle r_{n+p}^2 \rangle$$

$$\sigma_R^n = C \langle r_n^2 \rangle$$

$$\sigma_R^p = C \langle r_p^2 \rangle$$

with C from theory



H.Lenske, P.Kienle  
 $t_p = t_n$ , T.Elioff et al.  
 Phys.Rev.  
 128,869,(1962)<sub>9</sub>

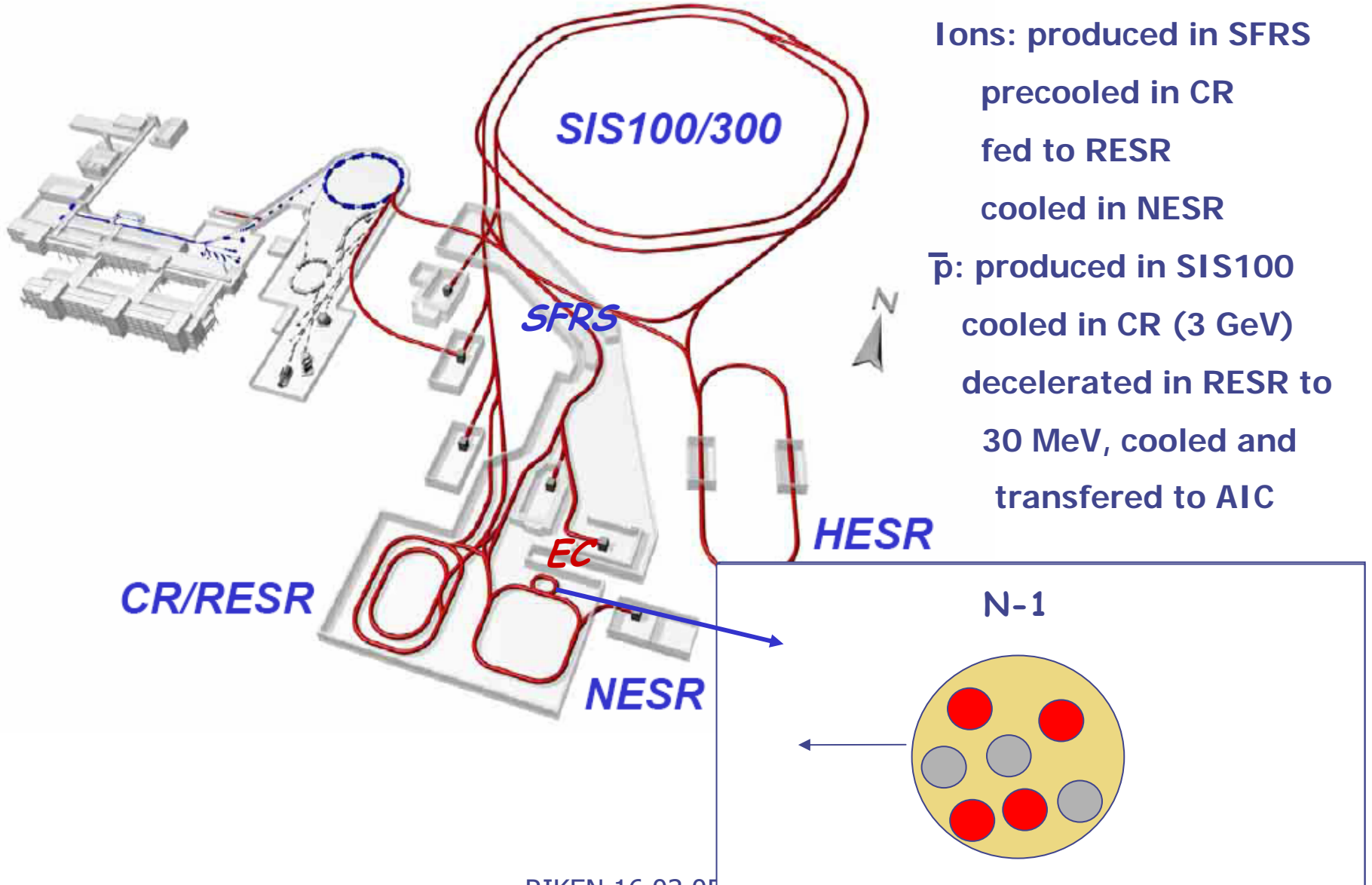


# Determination of Parameters of Fermi Distribution: $c_n, a_n; c_p, a_p$

- The energy dependence of  $\sigma_n(T)$  and  $\sigma_p(T)$  can be measured
- At high T crosssections are determined by  $c_n$  and  $c_p$  respectively
- At low T the tails of the Fermi distributions contribute
- The cross sections at low T are determined by  $c_n$  and  $a_n$ , and  $c_p$  and  $a_p$
- A detailed analysis of  $\sigma_n(T)$  and  $\sigma_p(T)$  is in progress



# The Idea of AIC in FAIR

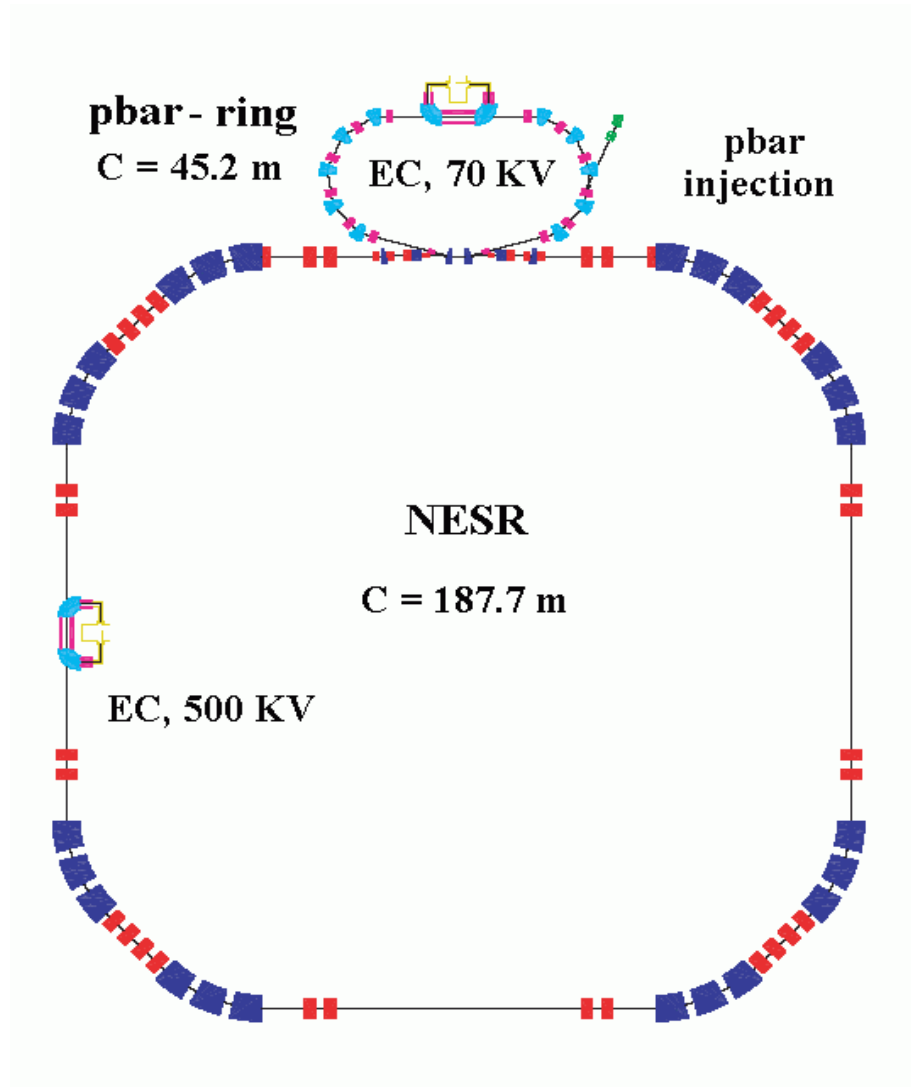


Ions: produced in SFRS  
precooled in CR  
fed to RESR  
cooled in NESR

$\bar{p}$ : produced in SIS100  
cooled in CR (3 GeV)  
decelerated in RESR to  
30 MeV, cooled and  
transferred to AIC

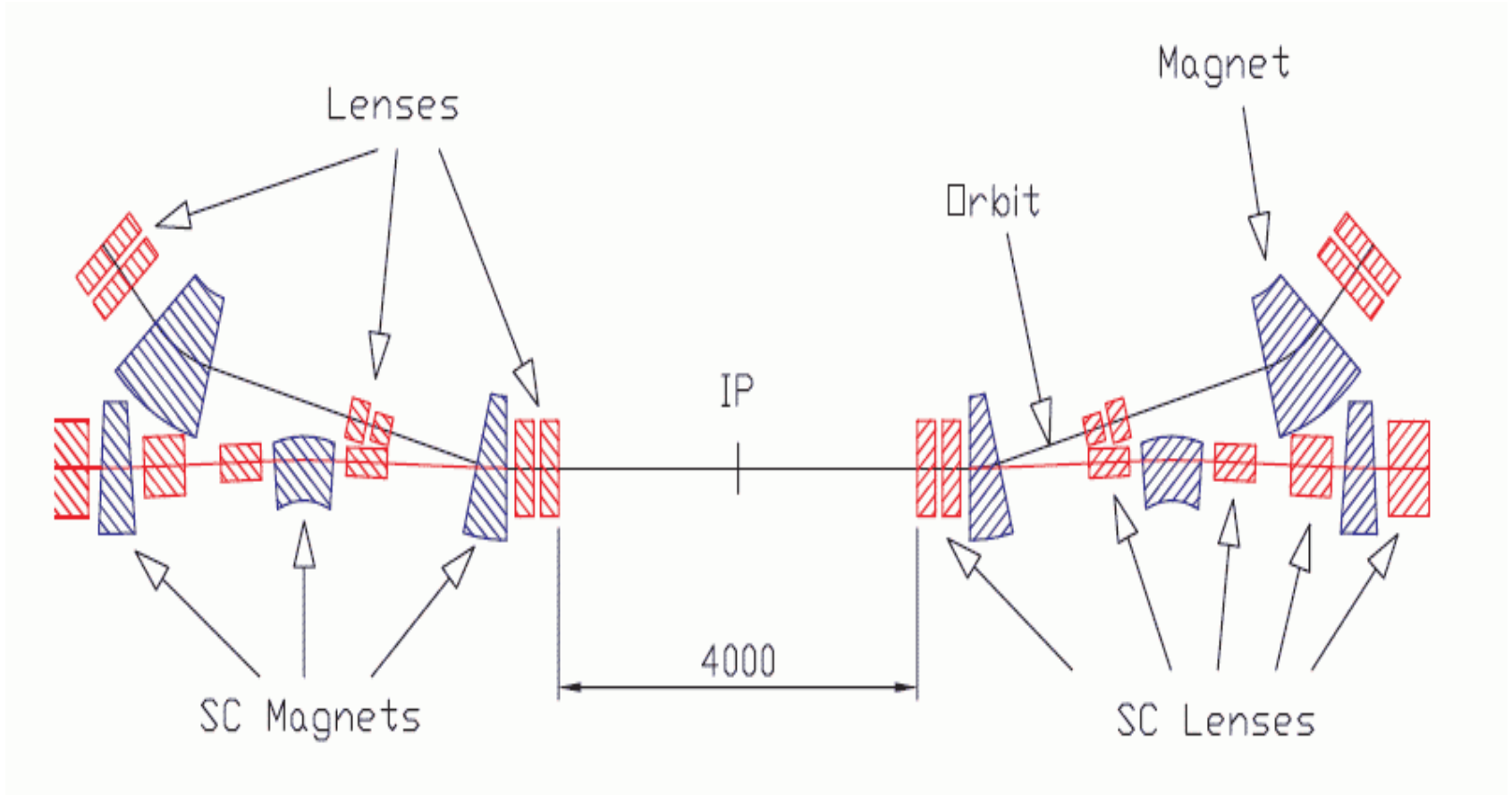


# AIC Conceptual Design



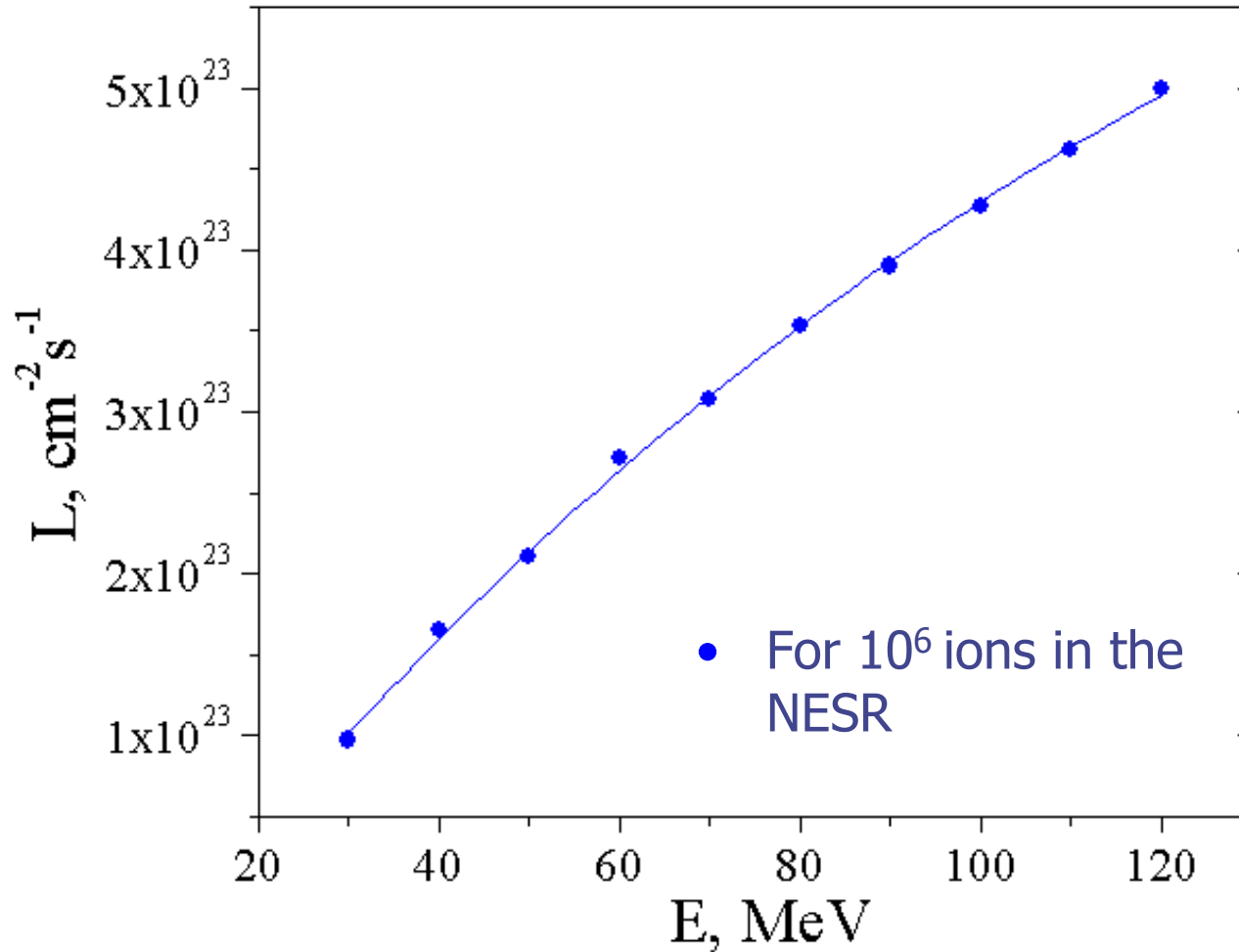


# AIC Interaction Zone





# AIC Luminosity, $L(E)$





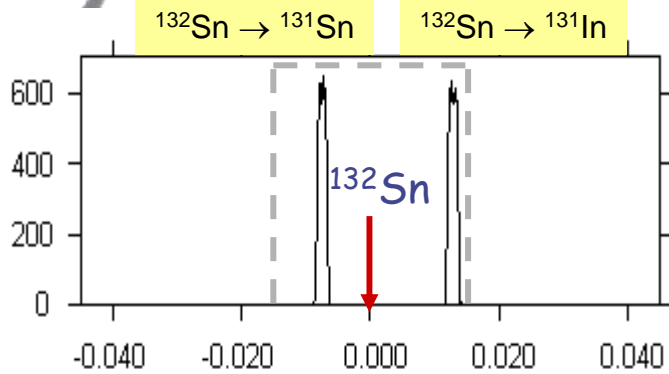
# Yield, Luminosity, Measuring Time

- Using continuous longitudinal stacking:  $N_s = \tau(dN/dt)$

Ion	$T_{1/2}$	yield	Luminosity	Time for $10^4$ events
$^{52}\text{Ca}$	12s	$4 \cdot 10^5$ pps	$5 \cdot 10^{23} \text{cm}^{-2} \text{s}^{-1}$	~300 min
$^{55}\text{Ni}$	0.5s	$8 \cdot 10^7$ pps	$4 \cdot 10^{24} \text{cm}^{-2} \text{s}^{-1}$	~35 min
$^{134}\text{Sn}$	2.7s	$8 \cdot 10^5$ pps	$2 \cdot 10^{23} \text{cm}^{-2} \text{s}^{-1}$	~360 min
$^{187}\text{Pb}$	34s	$1 \cdot 10^7$ pps	$3 \cdot 10^{25} \text{cm}^{-2} \text{s}^{-1}$	~2 min



# P/q Distributions of A-1 Nuclei

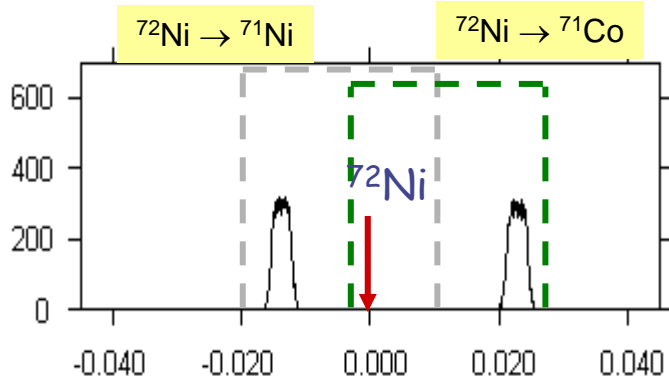


$A \sim 130$ :

$A$  & both  $A-1$  nuclei in the acceptance

$\Rightarrow$  Schottky method using one ring setting

$\Rightarrow$  recoil detection

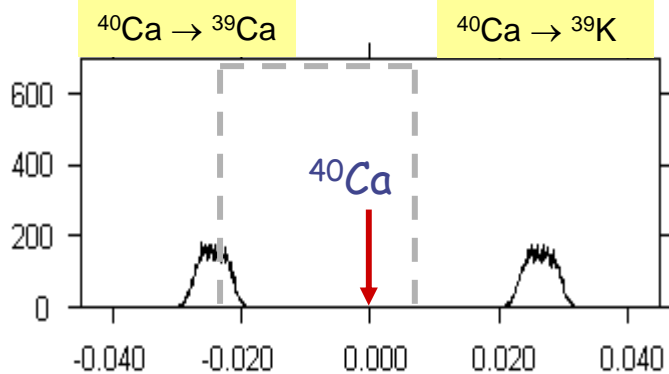


$A \sim 70$ :

$A$  & one  $A-1$  nucleus in the acceptance

$\Rightarrow$  Schottky method using two ring settings

$\Rightarrow$  recoil detection



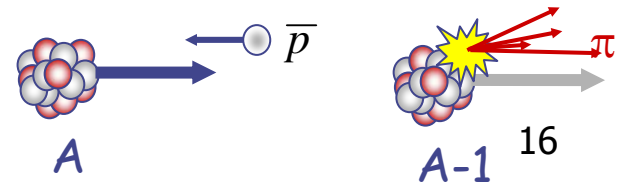
$A < 60$ :

$A-1$  nucleus not in the acceptance

$\Rightarrow$  recoil detection

$\epsilon_z$

RIKEN 16.03.05 P. Kienle





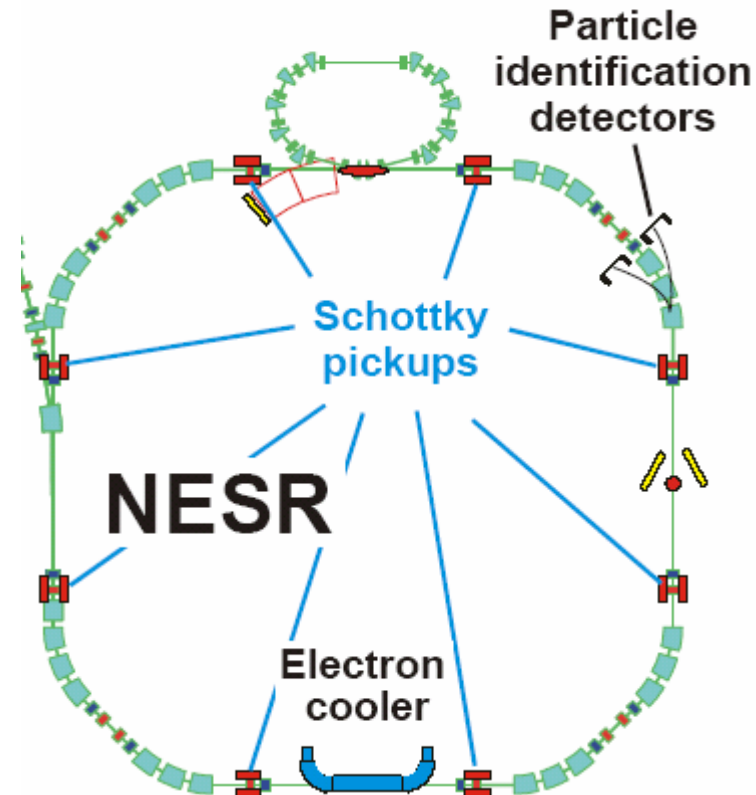
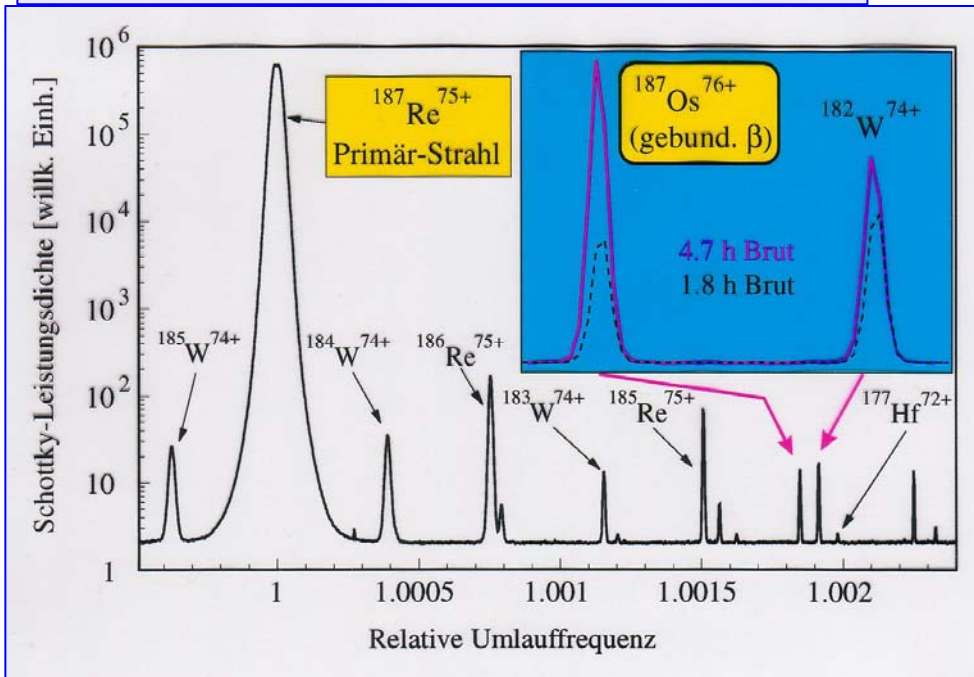
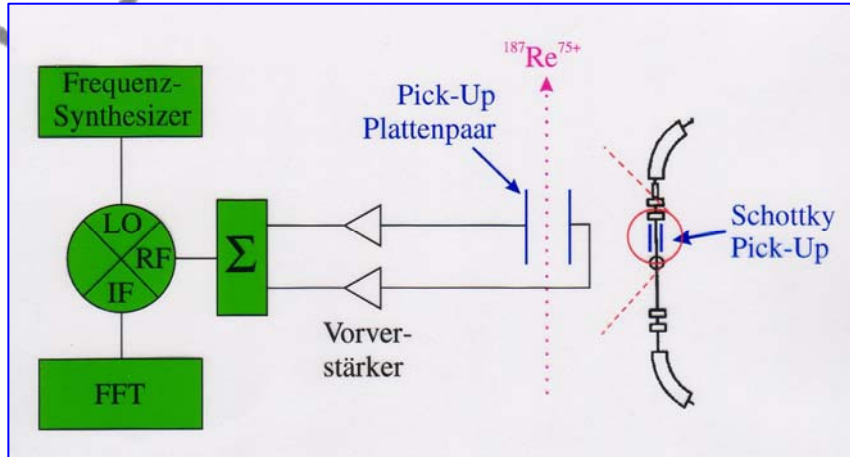


# Momentum Distribution of A-1 Nuclei

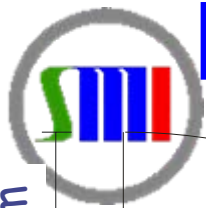
- Experiments at LEAR showed that the antiproton is a quasielastic process
- The recoil momentum distribution reflects the momentum distribution of the absorbed neutron or proton
- The recoil momentum distribution can be measured by magnetic spectrometry and Schottky spectroscopy



# Schottky Detection of Recoils



# Recoil Detection after dipole section



Staged set of recoil detectors covers large momentum range

0.5 m

5 m

+7%  
-6%

Existing ESR detector (TUM)

X-strip detector  
(140  $\mu\text{m}$ , 22x63mm<sup>2</sup>)

Y-strip detector  
(500  $\mu\text{m}$ , 22x54mm<sup>2</sup>)

6 Si-PIN-Diodes  
(1000  $\mu\text{m}$ , 38x54mm<sup>2</sup>)

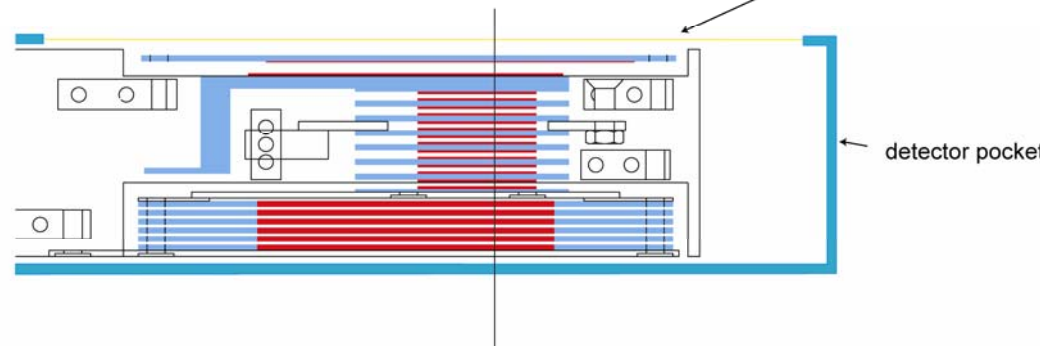
14 Si-PIN-Diodes  
(400  $\mu\text{m}$ , 20x20mm<sup>2</sup>)

37 mm

57 mm

Fe-window(50  $\mu\text{m}$ , 40x120mm<sup>2</sup>)

Position resolution  
better than 0,3 mm  
+ energy loss  
measurement

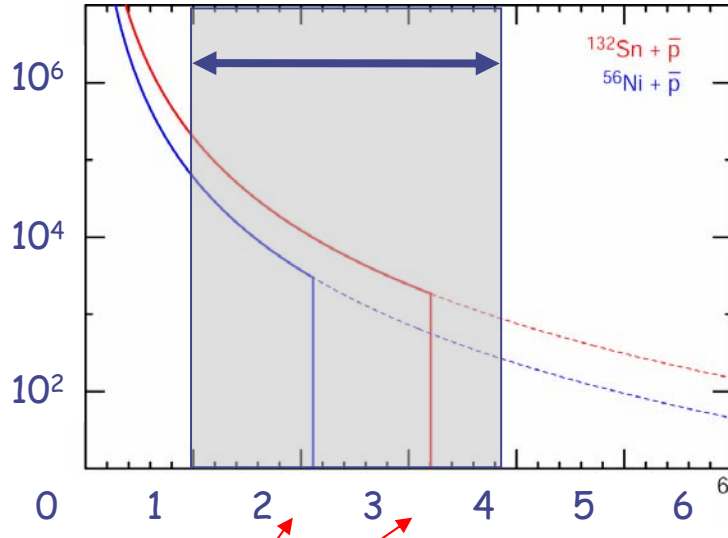




# Luminosity Measurement

Diff. Cross-section [b/sr]

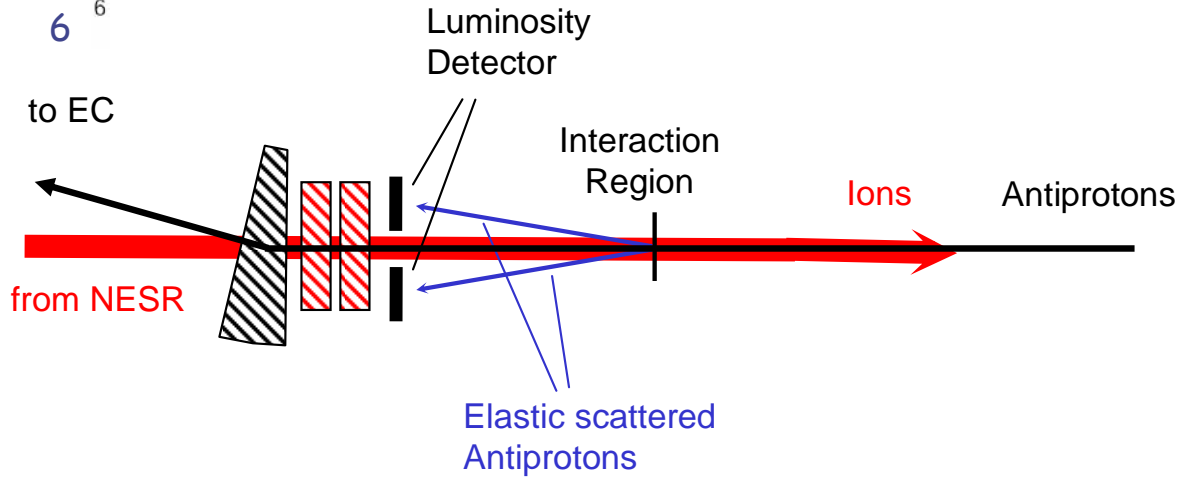
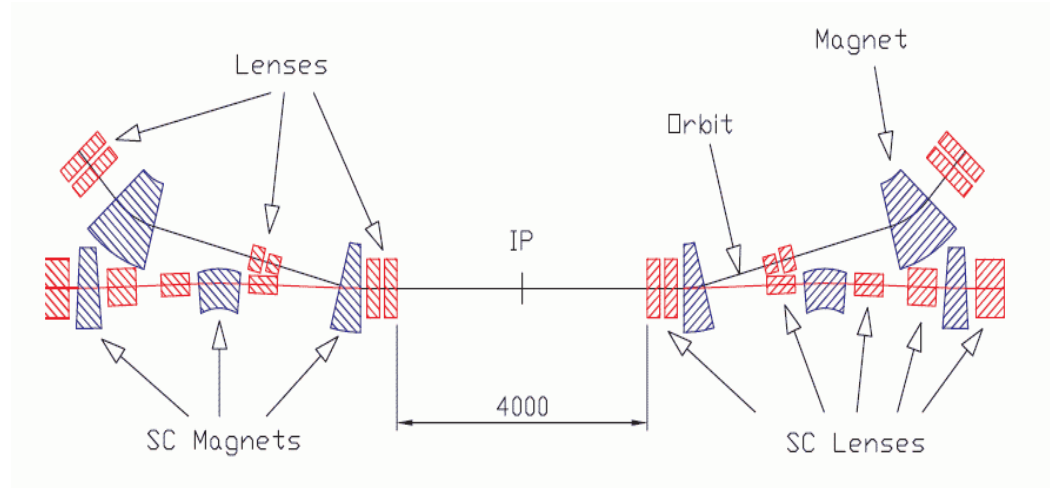
detector



$\theta_{lab}$  [degrees]

Grazing angle

$$Ldt = - \frac{dN_{elast}}{\sigma_{elast}}$$





# X-Sections and MS Radii

Luminosity from elastic scattering

$$Ldt = -\frac{dN_{\text{elast}}}{\sigma_{\text{elast}}}$$

Total reaction cross-section  
from reduction of primary ions  
with mass A

cross-section for production  
of A-1 nuclei:

$$\sigma_T = -\frac{dN_R}{Ldt}$$

$$\sigma_{i=n,p} = \varepsilon_{(A-1,i)} \cdot \frac{dN_{(A-1,i)}}{Ldt}$$

$$\sigma_T = C \langle r_{n+p}^2 \rangle = x(\sigma_n + \sigma_p)$$

$\varepsilon_{(A-1,i)}$  Detection efficiency  
for A-1 nuclei

exp. determined loss-factor

$$x = \frac{(\sigma_n + \sigma_p)}{\sigma_T}$$

$$x(\sigma_n + \sigma_p) = C(\langle r_n^2 \rangle + \langle r_p^2 \rangle)$$

$$\langle r_n^2 \rangle = \frac{x}{C} \sigma_n$$

$$\langle r_p^2 \rangle = \frac{x}{C} \sigma_p$$

$$\frac{\langle r_n^2 \rangle}{\langle r_p^2 \rangle} = \frac{\sigma_n}{\sigma_p}$$



# AIC Physics Program

- **Benchmarking: radii for the Sn isotopic chain**
  - stable isotopes, measured with different techniques
  - plan: extending from  $^{105}\text{Sn}$  to  $^{135}\text{Sn}$
- Radii along other closed-shell isotopic and isotonic chains
- Radii for nuclei near the drip-line in light nuclei
  - transition from halo nuclei to neutron skins
- Behaviour of radii across a shape transition
  - e.g. from  $^{80}\text{Zr}$  to  $^{104}\text{Zr}$
- Odd-even effects in nuclear radii
- Study the antiproton-neutron interaction



# Summary and Outlook

- Antiproton-nucleus cross section at 740 MeV/u is proportional to  $\langle r^2 \rangle$
- Detection of A-1 products allows
  - determination of proton and neutron radii
  - in the same experiment (same systematic uncert.)
  - in a model independent way
  - parameters of Fermi distribution from energy dependence
- AIC is feasible in terms of technology and physics output
- Simple counting experiment using Schottky method or recoil detectors (once the collider runs)
- AIC allows systematic investigation of
  - Neutron skins
  - Transition from halos to skins
  - Odd-even staggering in radii
  - Shape coexistence and its effect on neutron and proton radii
  - Nucleon-antiproton interaction



# AIC Collaboration

## Antiproton-Ion Collider Collaboration



- Spokesperson / Deputy: R. Krücken<sup>C</sup> / J. Zmeskal<sup>A</sup>
- Project Manager / Deputy: P. Kienle<sup>C</sup> / L. Fabbietti<sup>C</sup>

Beller, Peter <sup>A</sup>  
Bosch, Fritz<sup>A</sup>  
Cargnelli, Michael<sup>B</sup>  
Fabbietti, Laura <sup>C</sup>  
Faestermann, Thomas<sup>C</sup>  
Frankze, Bernhard<sup>A</sup>  
Fuhrmann, Hermann<sup>B</sup>  
Hayano, Ryugo S.<sup>D</sup>  
Hirtl, Albert<sup>B</sup>  
Homolka, Josef<sup>C</sup>  
Kienle, Paul<sup>B,C</sup>  
Kozhuharov, Christophor <sup>A</sup>

Krücken, Reiner<sup>C</sup>  
Lenske, Horst<sup>E</sup>  
Litvinov, Yuri <sup>A</sup>  
Marton, Johann<sup>B</sup>  
Nolden, Fritz <sup>A</sup>  
Ring, Peter<sup>C</sup>  
Shatunov, Yuri <sup>F</sup>  
Skrinsky, Alexander N. <sup>F</sup>  
Suzuki Ken, <sup>C</sup>  
Vostrikov, Vladimir A. <sup>F</sup>  
Yamaguchi, Takayuki <sup>G</sup>  
Widmann, Eberhard <sup>B</sup>  
Wycech, Slawomir <sup>H</sup>  
Zmeskal, Johann<sup>B</sup>

Institute A, Gesellschaft für Schwerionenforschung, Darmstadt, Germany (GSI)  
Institute B, Stephan Meyer Institut, Vienna, Austria (SMI)  
Institute C, Technische Universität München, Munich, Germany (TUM)  
Institute D, University of Tokyo, Tokyo, Japan (UoT)  
Institute E, Justus-Liebig Universität Giessen., Giessen, Germany (JLU)  
Institute F, Budker Institute of Nuclear Physics, Novosibirsk, Russia (BINP)  
Institute G, University of Saytama, Saytama, Japan.(UoS)  
Institute H, Andrzej Soltan Institute for Nuclear Studies, Warsaw, Poland (IPJ)





# Antiproton optical potential

$$f_{\bar{p}N}(T_{Lab}, q) = \frac{ik}{4\pi} \sigma_{\bar{p}N}(T_{Lab}) (1 - i\epsilon) F_{\bar{p}N}(q^2)$$

$$F_{\bar{p}N}(q^2) = e^{-\beta^2 q^2}$$

$$t_{\bar{p}N}(T_{Lab}, q^2) = \frac{2\pi\hbar}{M} f_{\bar{p}N}(T_{Lab}, q^2)$$

$$U_{opt}(\mathbf{r}) = \sum_{N=p,n} \int \frac{d^3q}{2\pi^3} \rho_N(q) t_{\bar{p}N}(T_{Lab}, q^2) e^{i\mathbf{q}\cdot\mathbf{r}}$$

$$U_{opt} = U_c + V + iW$$



# Cross Section

$$\left( -\frac{\hbar^2}{2\mu} \nabla^2 + U_{opt} - T_{lab} \right) \Psi^{(+)}(\mathbf{k}, \mathbf{r}) = 0$$

$$\Psi^{(+)}(\mathbf{k}, \mathbf{r}) \rightarrow e^{i\mathbf{k}\cdot\mathbf{r}} + f_{pA}(\hat{k}) \frac{e^{ikr}}{r} \quad S_{\ell j} = \eta_{\ell j} e^{2i\delta_{\ell j}}$$

$$\sigma_{abs}(\ell j) = \frac{4\pi}{k^2} \frac{2j+1}{2s+1} (1 - |S_{\ell j}|^2) = \frac{4\pi}{k^2} \frac{2j+1}{2s+1} (1 - \eta^2)$$

$$\sigma_{abs} = \sum_{\ell j} \sigma_{abs}(\ell j)$$

$$\sigma_{abs} = \frac{4\pi}{k} \int d^3r \Psi^{(+)\dagger}(\mathbf{k}, \mathbf{r}) \frac{-2\mu}{\hbar^2} \Im U_{opt}(\mathbf{r}) \Psi^{(+)}(\mathbf{k}, \mathbf{r})$$

$$\sigma_{abs}^{(q)} = \frac{4\pi}{k} \int d^3r \Psi^{(+)\dagger}(\mathbf{k}, \mathbf{r}) - \frac{2\mu}{\hbar^2} W^{(q)}(\mathbf{r}) \Psi^{(+)}(\mathbf{k}, \mathbf{r})$$